

# GNSS Permanent Station Data Analysis in Crustal Deformation Studies

**Riccardo Barzaghi and Barbara Betti**

*DICA-Politecnico di Milano, Piazza Leonardo da Vinci 32, 20133-Milano*

**Abstract:** Crustal deformation analysis in seismogenic areas is one of the most important applications of GNSS. In the last twenty years, the GNSS technology has opened new perspectives in this field allowing the estimation of the crustal deformation at different scales both in time and in space.

Tectonic deformations can be reliably estimated either at regional and fault scale. This allows the analysis of the different phases of the seismic cycle. Particularly, co-seismic and post-seismic deformations can be properly evaluated. Also, recent studies aim at studying the inter-seismic phase giving important insights in the dynamic of the crust in seismic prone areas.

These studies are commonly based on the analysis of time series from GNSS permanent stations. In this paper, a new method for filtering these data is presented and a case study based on the FReDNet data is illustrated.

## 1. Introduction

The analysis of crustal deformations plays an important role in studies related to the whole seismic cycle. Co-seismic, post-seismic and inter-seismic crustal deformations can be reliably estimated using daily coordinates time series from GNSS permanent stations. Many seismogenic areas are monitored in this way. As an example, one can mention the Southern California Integrated GPS Network (SCIGN) that has been completed in 2001 and consists of more than 250 stations (Figure 1, Hudnut et al, 2002).

GNSS permanent stations for deformation analysis are carefully monumented to properly detect crustal deformations. Deep-drilled brace are frequently used in order to couple the GNSS antenna to ground in a stable way (Figure 2).

In Italy, the Istituto Nazionale di Geofisica e Vulcanologia (INGV) has established the Rete Integrata Nazionale GPS (RING) with more than 180 stations (Figure 3, Avallone et al., 2010) and the Istituto Nazionale di Oceanografia e di Geofisica Sperimentale (OGS) has implemented the FReDNet in the North-East Alpine area (Figure 4, Zuliani et al, 2002).

*Quod Erat Demonstrandum – In quest of the ultimate geodetic insight |*

Special issue for Professor Emeritus Athanasios Dermanis |

School of Rural and Surveying Engineering, AUTh, 2018

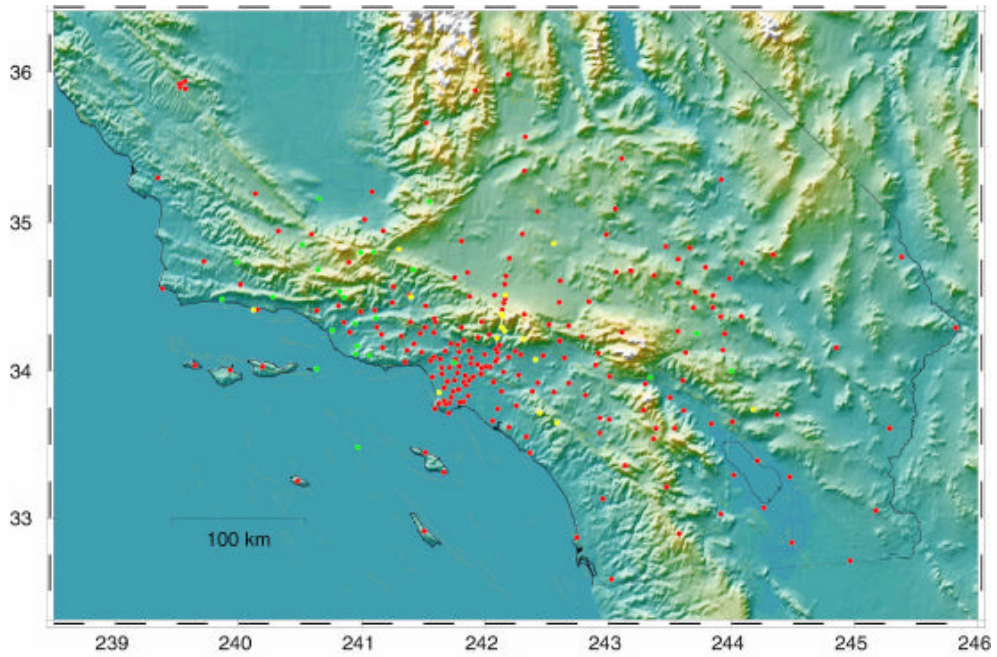


*Figure 1. The SCIGN network (status September, 2000)*

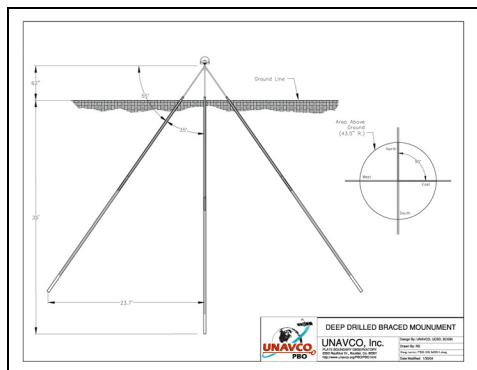


*Figure 2. The deep drilled brace*

Besides a careful monument setting, a detailed data analysis must be carried out in order to properly estimate the crustal movements.

The most common parametric model that is used in analysing the coordinate components  $\underline{X} = (x_1, x_2, x_3) = (N, E, Up)$  of the GNSS daily time series is

$$x_i = a + bt + \sum_{k=1}^N [A_k \cos(\omega_k t) + B_k \sin(\omega_k t)] + \sum_{j=1}^M c_j H(t - t_j) + \varepsilon_i(t) \quad i = 1, 2, 3 \quad (1.1)$$



*Figure 3. The RING network*

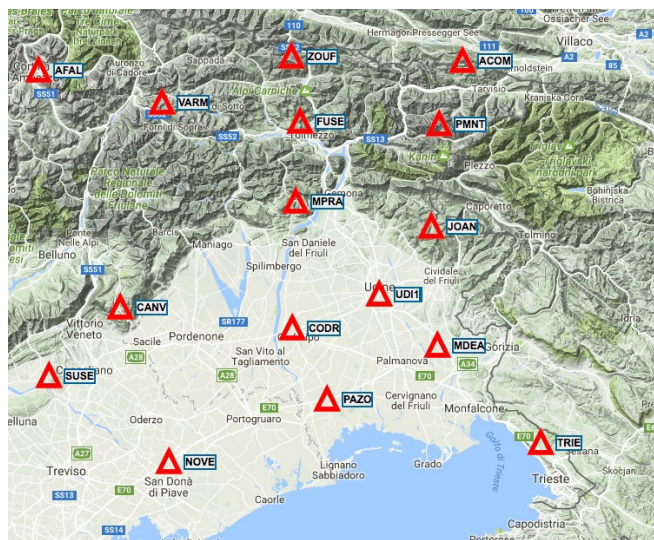


*Figure 4. The FReDNet network*

This model has been proposed by different authors (see e.g. Nikolaidis, 2002). The linear term accounts for the station velocity while harmonic components are included to model annual, seasonal and higher frequency time dependent phenomena. Possible discontinuities due to instrument/software and/or reference frame changes are modelled by the terms containing the Heaviside function  $H(\cdot)$ . By least squares adjustment, the model parameters are estimated assuming different models for the coloured noise  $\varepsilon_i(t)$ . The most common stochastic models for  $\varepsilon_i(t)$  are those presented in Williams (2003) with further implementations in Williams (2008). In these papers  $\varepsilon_i(t)$  is assumed to have a power spectrum that depends on the frequency  $f$  according to the formula

$$P(f) \approx f^k \quad (1.2)$$

Based on the value of  $k$ , different stochastic process can be described with this model. If  $k$  is in the range  $-1 \leq k \leq 1$ ,  $\varepsilon_i(t)$  is a stationary stochastic process. For  $|k| > 1$   $\varepsilon_i(t)$  is non-stationary (Mandelbrot 1967). Particular cases are for  $k=0$ ,  $k=-1$  and  $k=-2$  for which the  $\varepsilon_i(t)$  process is, respectively, a White Noise process, a Flicker Noise process or a Random Walk process.

A different time-domain approach has been proposed by Barzaghi et al. (2004) where  $\varepsilon_i(t)$  is assumed to be a second order stationary process, ergodic in the covariance.

In this case, the parameters estimation is done in a two steps procedure. The first least squares iteration is accomplished by considering that  $\varepsilon_i(t)$  is White Noise. The  $\varepsilon_i(t)$  least squares residuals are then computed and their stationarity is tested using the generalized KPSS-test (Hobijn et al., 2004). If stationarity condition is satisfied (which currently happens in the authors' experience when removing the linear, annual and semi-annual terms in (1.1)), the empirical auto-covariance of  $\varepsilon_i(t)$  is estimated and then modelled with a proper positive definite model function. Least squares adjustment is then repeated using the derived covariance structure.

Furthermore, using this concept, collocation can be applied for filtering the residuals  $\varepsilon_i(t)$ . This can be done in order to detect and describe possible high frequency effects that are present in the GNSS coordinates time series (Borghi et al., 2016). In the following this filtering approach is detailed and applied to GNSS coordinate time series of the FReDNet network.

## 2. Filtering the GNSS time series

The filtering procedure of the GNSS coordinate time series that is proposed in this paper is developed in subsequent steps. At first, a usual outliers rejection is set up and known discontinuities due to e.g. instrumental changes are removed (see Figure 5).

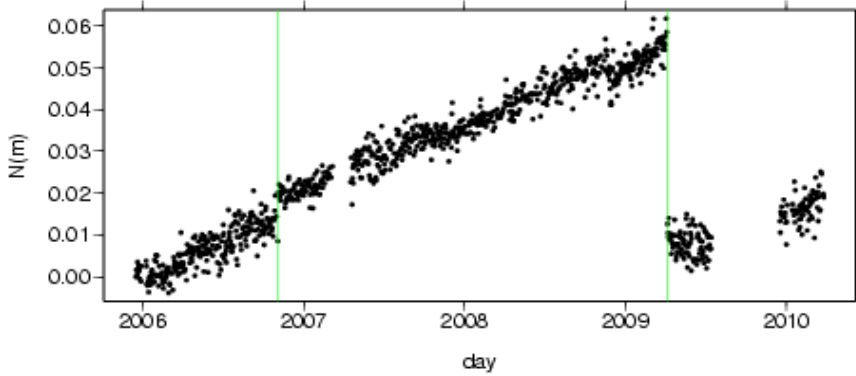


**Figure 5.** Discontinuities in GNSS time series

The parametric model (1.1) is then estimated assuming White Noise behaviour of  $\varepsilon_i(t)$ . Least squares residuals are then checked for stationarity by means of KPSS test. As already stated, using a proper parametric model stationarity of the residuals is ensured. The empirical auto-covariance function is then estimated and fitted with a proper model covariance function, i.e. a positive definite function, as in Figure 6.

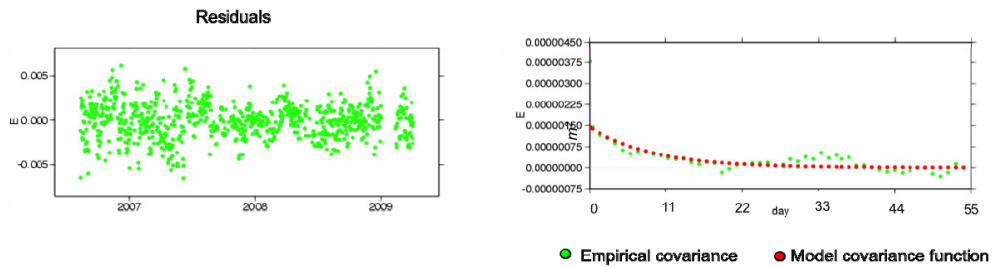


**Figure 6.** The least squares residuals, the empirical covariance function and the best-fit model

The final estimate of the model parameters is then accomplished in a further least square step that is performed using the proper covariance structure as defined by the model covariance function. Thus, the parametric model is optimally estimated taking into account the existing time correlations (see Figure 7).

Starting from the second step least squares residuals, a filtering procedure can be applied. We assume that the residuals  $\varepsilon_i(t)$  can be modelled as the sum of a time correlated weakly stationary signal  $s_i(t)$  and a white noise (uncorrelated) component  $n_i(t)$ , independent from  $s_i(t)$

$$\varepsilon_i(t) = s_i(t) + n_i(t) \quad i = 1, 2, 3 \quad (2.1)$$

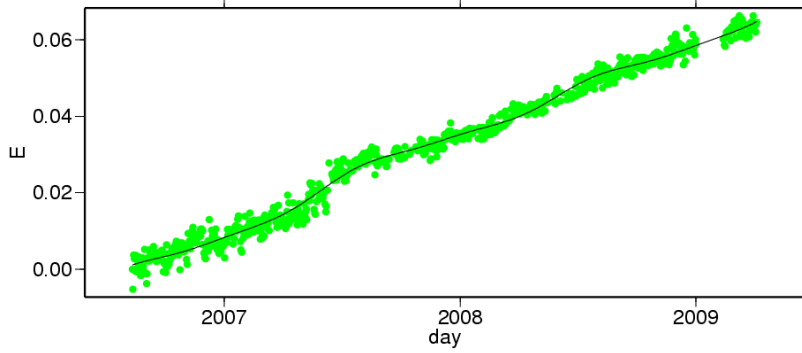


**Figure 7.** *The best-fit parametric model*

As already pointed out, under these hypotheses, the empirical covariance function of  $\varepsilon_i(t)$  can be estimated and modelled. Collocation filtering method (Moritz, 1980) can be applied to the residuals in order to estimate the signal component as

$$\hat{s}_i(t) = \sum_{j,k=1}^N C(|t-t_k|) [C + \sigma_n^2 I]_{kj}^{-1} \varepsilon_j(t_j) \quad i=1,2,3 \quad (2.2)$$

The filtered component allows defining some coherent behaviour of the residuals that could be related to some crustal deformations (see Figure 8).

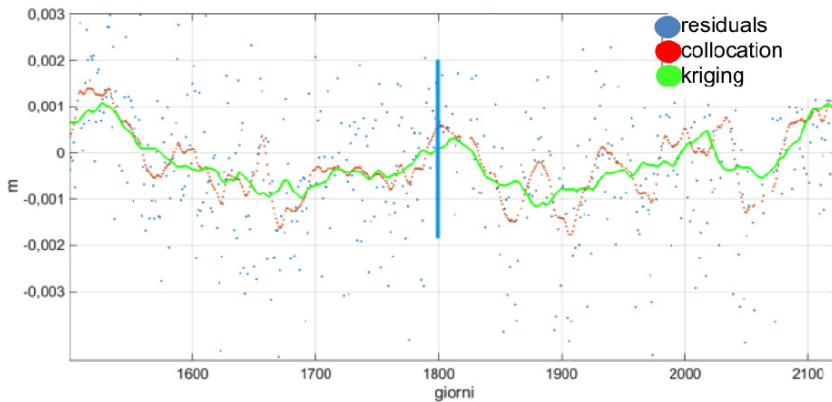


**Figure 8.** *The least squares residuals and the filtered signal*

Although this filtering procedure is quite effective, a further smoothing could be required to enhance the low frequency components of the filtered signal. It is in fact expected that possible inter-seismic crustal deformations have a smooth behaviour in time. In order to enhance the low frequency component in  $\hat{s}_i(t)$ , a moving average operator can be applied. As it is well known this is equivalent to low pass filtering in the frequency domain (Bracewell, 1986).

This low-pass filtering procedure can be accomplished by kriging moving average (Wackernagel, 2003). We considered an amplitude of the sliding time window equal to twice the correlation length of the covariance function  $C(\cdot)$  of  $\hat{s}_i(t)$  (the correlation length is the distance at which the covariance function is half its value in the origin). The mean value of the signal over this sliding window is computed as

$$\hat{m}_s = \sum_{j=1}^N \omega_j \hat{s}_i(t_j) \quad i=1,2,3 \quad (2.3)$$

where  $N$  is the number of  $\hat{s}_i(t)$  values in the window and the  $\omega_k$  weights are given as the solution of the system

$$\begin{cases} \sum_{j=1}^N \omega_j C(t_i - t_j) - \eta = 0 \\ \sum_{j=1}^N \omega_j - 1 = 0 \end{cases} \quad i=1, \dots, N \quad (2.4)$$

The low pass-filtered signal is thus smoother than the original values as it is shown in Figure 8 (green line).

By using such regularized residuals, analyses on possible transient crustal deformations can be performed effectively since most of the noise sources have been eliminated from the  $\varepsilon_i(t)$  residuals. In the following section, the application of this procedure to the FReDNet GNSS time series is discussed.

### 3. The FReDNet case study

The FReDNet network, as already mentioned, is a GNSS network which has been established for estimating the crustal deformation in the Eastern Alpine area. Most of the stations have been recording data for a long time period. In our analysis, we selected thirteen stations that have more than three years of data. They are plotted in Figure 9 (red stations) together with those having a shorter acquisition period (white stations).

The filtering procedure described in Section 2 has been applied to the coordinate components of each station and the filtered residuals in (2.3) have been estimated. In order to investigate if spatially correlated phenomena can be seen in these values, the Principal Component Analysis (PCA) has been applied (Jolliffe, 2002). This analysis has been performed on the horizontal components only. For each component, the following matrix  $Y^k$  has been set up

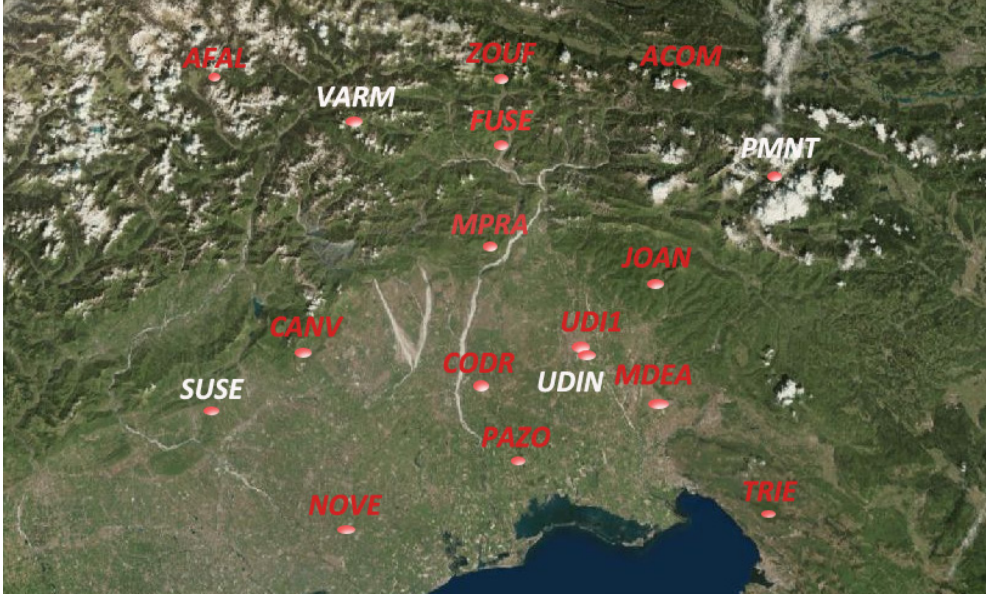


**Figure 9.** The stations selected for the analysis (in red)

$$Y^k = \begin{bmatrix} \hat{m}_1^k(t_1) & \hat{m}_2^k(t_1) & \dots & \hat{m}_p^k(t_1) \\ \hat{m}_1^k(t_2) & \hat{m}_2^k(t_2) & \dots & \hat{m}_p^k(t_2) \\ \vdots & \vdots & \ddots & \vdots \\ \hat{m}_1^k(t_N) & \hat{m}_2^k(t_N) & \dots & \hat{m}_p^k(t_N) \end{bmatrix} = \begin{bmatrix} y_{11}^k & y_{12}^k & \dots & y_{1p}^k \\ y_{21}^k & y_{22}^k & \dots & y_{2p}^k \\ \vdots & \vdots & \ddots & \vdots \\ y_{N1}^k & y_{N2}^k & \dots & y_{Np}^k \end{bmatrix} \quad (3.1)$$

where  $k$  is the component index ( $k=1$  for the North component and for  $k=2$  for the East component),  $p$  is the number of considered stations and  $N$  the number of days in the time series ( $N > p$ ). By Singular Value Decomposition (SVD) of  $Y^k$  one can get

$$Y^k = U^k L^k (V^k)^t \quad (3.2)$$

where  $U^k$  and  $V^k$  are suitable orthogonal matrices and  $L^k$  is a diagonal matrix having dimension equal to the rank  $r$  of  $Y^k$ . The columns of  $U^k$  and  $V^k$  are called left and right singular vectors for  $Y^k$  and the diagonal elements in  $L^k$  are called singular values of  $Y^k$ .

By virtue of (3.2), one can write for each component of (3.1)

$$y_{ij}^k = \sum_{m=1}^r u_{im}^k l_m^k v_{jm}^k \quad (3.3)$$



Also, by considering only the first most relevant  $m < r$  singular values one can obtain the approximation of the elements of  $Y^k$  as

$$(\tilde{y}_{ij}^k)^m = \sum_{n=1}^m u_{in}^k l_n^k v_{nj}^k \quad (3.4)$$

The PCA is intimately related to SVD of  $Y^k$  since it can be proved that  $U^k$ ,  $V^k$  and  $L^k$  define also a possible spectral decomposition of the covariance matrix of  $Y^k$ . Thus, by considering the larger  $m$  singular values one “explains” most of the variability contained in the covariance matrix of  $Y^k$ . In turn, by (3.4) one can also give an estimate of the signals implied by these singular values and see how they reproduce the original  $y_{ij}^k$  in (3.1). If some of the  $y_{ij}^k$  are properly reproduced using the selected larger singular values, one can also check if they are spatially clustered. In this way, by applying this analysis, one can find cluster of stations (if any) that mainly contribute to the overall variability. Since the signals considered in (3.1) refer to coordinate variations in time, this means that by virtue of this approach clusters of stations with “highly” variable coordinates can be found. Once we are able to detect these clustered stations, a cross-check can be performed with known seismic events and/or known fault systems which can account for this “high” coordinates variability.

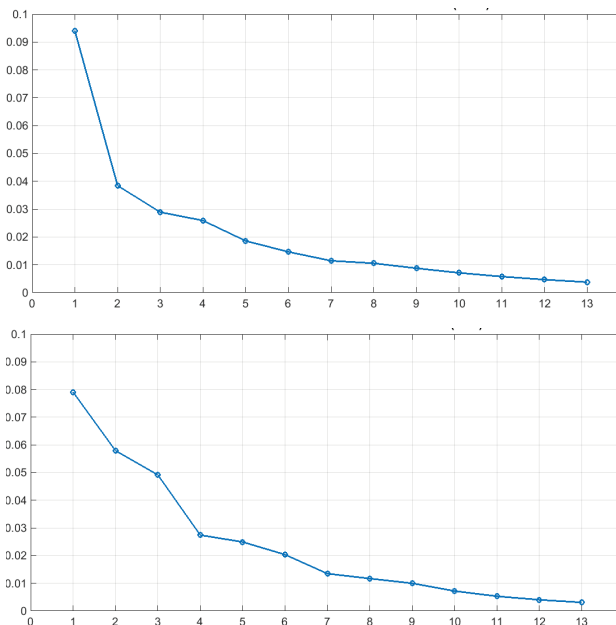


**Figure 10.** The PCA singular values for the considered FReDNet stations (North component on the left, East component on the right)

The PCA analysis on the selected stations led to the singular values that are plotted in Figure 10 for the North (left panel) and the East (right panel) components.

It can be seen that the first two values in each component are much larger than the remaining (this is particularly true for the North component). If we consider only these values, the signal in (3.4) can reproduce in a very detailed way that of one station only, namely the signal of the CANV station. In Figure 11, the CANV signal and its approximation (3.4) obtained with the first singular value are represented: the agreement of the two signals is striking.

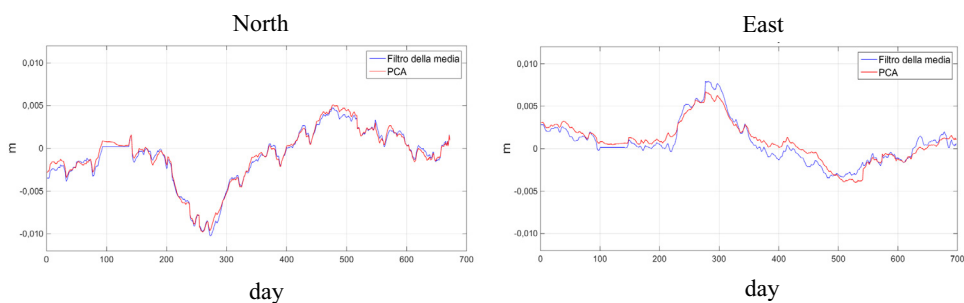


**Figure 11.** The PCA analysis on the CANV station signals (blue=original values; red=PCA signal)

The same doesn't hold for the remaining stations. As an example, the signals of the NOVE station are displayed in Figure 12.

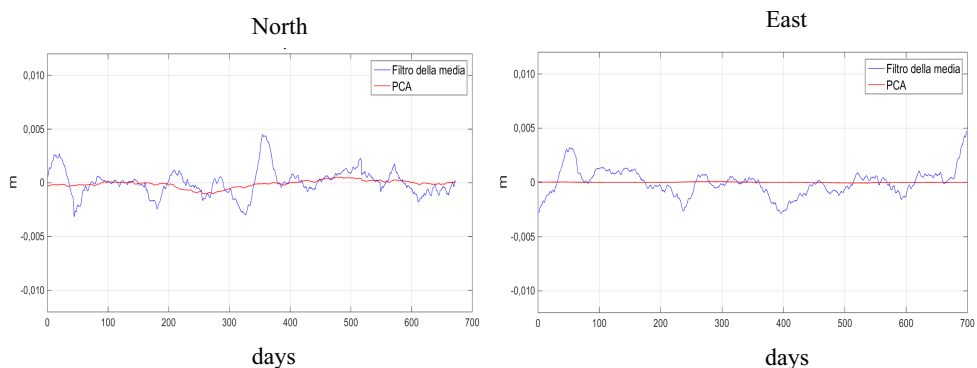


**Figure 12.** The PCA analysis on the NOVE station signals (blue=original values; red=PCA signal)

Thus, the main variation in the covariance matrices is then given by the CANV station. This means that, in the analysed period, this station has highly varying coordinates. In recent studies, it has been proved that this variability is given by a

local effect related to groundwater storage in the Cansiglio plateau area (Devoti et al., 2015). Hence, the proposed analysis proved to be effective since one physical phenomena was spatially related to a given station.

If we now remove the CANV station and repeat the same analysis on the twelve remaining stations, we have no sharp differences among the singular values. The filtered signals based on the larger singular values don't cluster so clearly in a specific area. There are however some (weak) indications of a better fit between the original signals and the filtered ones (using only the two larger singular values in each component) in the SE area (see Figure 13) where an earthquake occurred on December 6th, 2011 (the Gradisca d'Isonzo 0.8-magnitude seismic event).



**Figure 13.** The Gradisca d'Isonzo area and the FRedNet stations selected by the PCA analysis

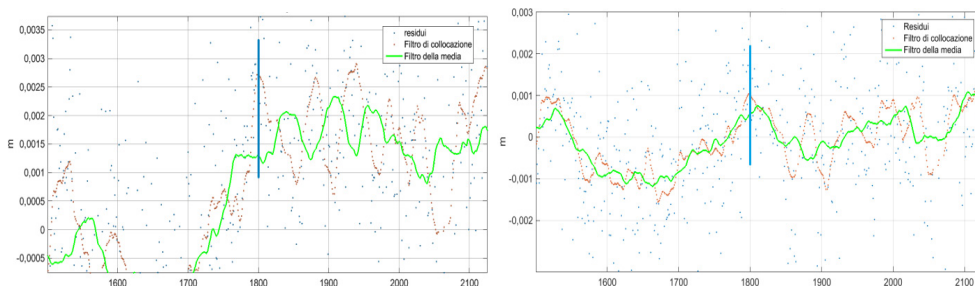


**Figure 14.** The TRIE (left panel) and MDEA (right panel) filtered East component residuals and the Gradisca d'Isonzo seismic event (blue line)

If the original signals of the stations clustered in the PCA analysis are inspected, one can see that on that date, some sharp variations are present. As an example, the East components of MDEA and TRIE (which are the closest stations to Gradisca d'Isonzo) are plotted in Figure 14. On December 6<sup>th</sup>, 2011 (blue line), they both display a common high signal variability.

#### **4. Conclusions**

In the last twenty years, GNSS technology has opened new perspectives in the geophysical investigations. Particularly, the crustal deformations can be nowadays estimated with high accuracy and precision. In this respect, an invaluable role is played by the GNSS permanent stations designed for monitoring crustal movements. The analysis of the coordinate time series allows describing the entire seismic cycle in seismogenic areas. The filtering procedure that has been designed in this paper proved to be effective and able to spatially cluster permanent stations having common behaviour. In the FReDNet case study, two different physical phenomena were identified. In the first analysis step, a groundwater storage effect in the Cansiglio area has been evidenced. The subsequent analysis allowed identifying a cluster of stations related to a 0.8-magnitude seismic event in the Gradisca d'Isonzo area. Further investigations are needed to prove that this procedure can reveal other geophysical relevant phenomena related to the inter-seismic phase such as, e.g., aseismic transient slip events.

#### **Acknowledgements**

The authors wish to thank Dr. David Zuliani and Dr. Giuliana Rossi of the National Institute of Oceanography and Experimental Geophysics (OGS) for providing the FReDNet GNSS time series data.

#### **References**

- Avallone, A., G. Selvaggi, E. D'Anastasio, N. D'Agostino, G. Pietrantonio, F. Riguzzi, E. Serpelloni, M. Anzidei, G. Casula, G. Cecere, C. D'Ambrosio, P. De Martino, R. Devoti, L. Falco, M. Mattia, M. Rossi, U. Tammara & L. Zarrilli (2010), The RING network: improvement of a GPS velocity field in Central Mediterranean, *Annals of Geophysics*, 53, 2
- Barzaghi, R., Borghi, A., Crespi, M., Pietrantonio, G., Riguzzi, F. (2004), GPS Permanent Network Solution: the Impact of Temporal Correlation. *International Association of Geodesy Symposia*, F. Sansò Eds., Vol. 127, 179-183.
- Borghi, A., Aoudia, A., Javed, F., Barzaghi, R. (2016), Precursory slow-slip loaded the

- 2009 L'Aquila earthquake sequence. GJI., doi: 10.1093/gji/ggw046
- Bracewell, R. N. (1986), *The Fourier Transform and its applications*. McGraw-Hill Book Company, New York.
- Devoti, R., Zuliani, D., Braitenberg, C., Fabris, P., Grillo, B., (2015), Hydrologically induced slope deformations detected by GPS and clinometric surveys in the Cansiglio Plateau, Southern Alps, *Earth and Planetary Science Letters* 419 (2015) 134-142, Elsevier.
- Hobijn, .B, Franses, P. H., Ooms, M. (2004), Generalization of the KPSS-test for stationarity. *Statistica Neerlandica*, 58, 4, 483-502.
- Hudnut K. W., Bock Y., Galetzka J. E., Webb F. H. and Young W. H. (2002), *The Southern California Integrated GPS Network (SCIGN)*. *Seismotectonics in Convergent Plate Boundary*, Y. Fujinawa and Y. Youshida Eds., Terra Scientific Publishing Company (TERRAPUB), Tokyo.
- Jolliffe, I. T., (2002), *Principal component analysis*. Springer-Verlag, New York, Berlin, Heidelberg, 2<sup>nd</sup> Edition.
- Mandelbrot, B. (1967), Some noises with 1/f spectrum, a bridge between direct current and white noise, *IEEE Transactions on Information Theory*, 13, 2, 289-298.
- Moritz, H. (1980), *Advanced Physical Geodesy*. Herbert Wichmann Verlag, Karlsruhe.
- Nikolaidis R (2002) *Observation of Geodetic and Seismic Deformation with the Global Positioning System*, PhD. Thesis.
- Zuliani, D., Battaglia, M., Murray, M., Marson, I. (2003), FReDNet: a Continuous GPS Geodetic Network Monitoring Crustal Deformation in NE Italy. *EOS*, Vol. 84, No 28.
- Wackernagel, H. (2003), *Multivariate Geostatistics: an Introduction with Applications*. Springer-Verlag, Berlin, 3<sup>rd</sup> edition.
- Williams, S. D. P. (2003), The effect of coloured noise on the uncertainties of rates estimated from geodetic time series, *Journal of Geodesy*, 76, 483-494.
- Williams, S. D. P. (2008) CATS: GPS coordinate time series analysis software. *Journal of Geodesy*, Volume 12, Number 2/March, DOI 10.1007/s10291-007-0086-4.